

# MICRO/MACRO APPROACH FOR PREDICTION OF MATRIX CRACKING EVOLUTION IN LAMINATED COMPOSITES

M.H. Ghayour<sup>1</sup>, H. Hosseini-Toudeshky<sup>1\*</sup>, M. Jalalvand<sup>2</sup> and Ever .J. Barbero<sup>3</sup>

<sup>1</sup>Department of Aerospace Engineering, Amirkabir University of Technology, Tehran, 424 Hafez Avenue Iran

<sup>2</sup> Advance Composite Centre for Innovation and Science, University of Bristol, Bristol BS8 1TR, UK

<sup>3</sup>Department of Mechanical and Aerospace Engineering, West Virginia University 6106, USA, 26506-6106

## Abstract

A computational constitutive model is presented to predict matrix cracking evolution in laminates under in-plane loading. Transverse cracks are treated as separate discontinuities in the micro model which provides damage parameters for the macro model. Both micro and macro models are implemented using Finite Element Analysis (FEA); specifically ANSYS, avoiding limitation of analytical micro modeling. The computational cost of the micro model is limited to constructing a database (DB) of micro-model predictions a priori. The macro-model is simply a FEA discretization of the structure using plane stress or shell elements in ANSYS. The macro model queries the DB, which effectively becomes a constitutive model. The damage surfaces in the DB are obtained from the results of large number of finite element micro-scale (unit-cell) analyses. The proposed procedure is implemented in ANSYS as a *usermaterial* subroutine for transverse crack initiation and propagation in symmetric cross-ply and  $[0_r/(\theta/-\theta)_s/0_n]_s$  laminates under in-plane loads. This method is also examined to study matrix crack evolution in tensile specimen with open hole and the results found to be in good agreement with available experimental data.

**Keywords:** Matrix damage, Matrix cracking, Multi-scale, Discrete fracture mechanics

## 1. Introduction

Damage analyses of composite laminates have been performed from nano to macro-scales. In the macro-scale analysis, effective homogenized material properties are used by the structural software (e.g., ANSYS) to find the deformations that are in equilibrium with the external loads, as well as prediction of damage progression and final failure. In the micro-scale analysis, cracks are modeled as explicit discontinuities to predict the crack density, stiffness, and stress that are compatible with the strain imposed by the macro-analysis at each Gauss point. Failure theories such as LaRC, Puck, Hashin, etc. can predict damage onset but are not able to track the evolution of damage. Continuum Damage Mechanics (CDM) has been employed by many researchers for progressive damage analyses of composite laminates, as

---

\*corresponding author: [hosseini@aut.ac.ir](mailto:hosseini@aut.ac.ir)

reviewed in <sup>1</sup>. However, the use of CDM alone requires additional material testing to adjust the empirical evolution laws. On the contrary, discrete fracture mechanics micro-models, such as <sup>2,3</sup> and the currently proposed one, do not use empirical evolution laws; the evolution is predicted by the model itself. Unlike <sup>2</sup>, which implements an analytical solution at the micro-scale, the model proposed in this paper is based on finite element analysis (FEA), but unlike coupled micro-macro FEA models, the proposed formulation performs the micro-model analyses a priori to train a database (DB), which is later queried by the macro-model. Populating the DB can be automated, and it is done a priori, once and for all <sup>4</sup>. This results in versatility and simplicity. Versatility is achieved because virtually unlimited configurations of damage modes can be analyzed by the micro-model due to the versatility of FEM itself. Simplicity accrues from the fact that the macro-model is a regular FEA discretization using commercially available software that, according to the proposed formulation, is able to query the DB to get the constitutive response.

Matrix cracking is often the first form of damage that occurs in composite laminates and its density usually increases up to a saturation state. Apart from stiffness reduction and accelerating the final failure, matrix cracking can cause other serious damages such as delamination and structure malfunction like leakage in pressure vessels. The stiffness reduction caused by matrix cracking has been studied by several analytical methods have been already developed for prediction of these effects. A variational approach for cross-ply laminates is presented in <sup>5</sup> and extended for thermal effects and angle ply laminates <sup>6-9</sup>. The Finite Element Method (FEM) has been also used to predict matrix crack formation as well as to find the stress distributions in the presence of micro-cracks by contributing the cohesive zone model<sup>10-12</sup>. Compared with analytical methods, FE based micromechanics models are not restricted to particular loading, boundary conditions, and geometry of the cracked region, for instance, matrix cracking at the free edges of tensile samples has been studied<sup>13</sup> using this approach. However, these micromechanics models are considerably more time-consuming, and thus more difficult to implement in a coupled micro/macro model where the micro-model is executed at every Gauss point and every iteration.

Existing analytical micromechanical models are restricted to simple loading conditions and geometries, but the excellent predictions achieved by these models make them worthy. An engineer prefers methods which are simple and robust. In these approaches damage characterization and damage evolution are usually performed at different scales. Usually, the micro-scale is homogenized for the macro-model to use it in a CDM approach. Multiscale methods have the advantages of both micro and macro mechanics methods. Micro-macro and micro-meso are two well-known categories in multi-scale approaches. Meso modeling, which is defined at ply level, is presented in <sup>14,15</sup>. A multi-scale model for matrix crack evolution in composite laminates is shown in <sup>16-18</sup>, where the material is described by means of two levels of layer and interface. In <sup>16-18</sup> the degraded material properties are represented as CDM to the macro FEA model, which finds the structural response of laminates under in-plane loading condition <sup>19</sup>.

A damage model using shear-lag approach in the micro-scale (unit-cell containing matrix cracks) was developed and implemented into discrete constitutive law at integration points of

a formulated shell element in macro model<sup>2, 20, 21</sup>. Using this approach it is possible to perform damage analyses for laminates containing discontinuities<sup>22</sup>. Synergistic damage mechanics merging crack opening displacement (COD) method and CDM is presented in<sup>23, 24</sup>. A model for cross-ply laminates based on the stress transfer method is presented in<sup>25</sup>, for general symmetric laminates under tensile/shear load embedded into a shell element using layer-wise theory and damage constitutive law<sup>26</sup>.

The primary goal of this manuscript is to present a multi-scale constitutive model where both micro and macro-level are based on the FE analysis. This will eliminate the need for analytical solutions in the micro-scale analysis and provide a generalized modelling approach in terms of boundary conditions and complicated configurations which is an important limitation in models based on analytical approaches. In most of the existing progressive matrix cracking methods, the damage evolution process consists of analytical methods restricted for certain types of damage, boundary conditions, and loading. In this paper, a new FE based micro-macro method is presented for predicting matrix crack damage evolution in composite laminates. Both the micro and macro models are based on FEA, but without running both models concurrently. Since the proposed model does not require analytical formulations and preventing repeated recalculation of the micro-model for each Gauss point and iteration makes the proposed method robust and a simple. Furthermore, both developed model and available experimental observations are examined in the room temperature. Thus, thermal residual stress which is a dominant factor in the critical strain energy release rate and consequently the matrix cracks initiation is taken into account in the model.

To demonstrate the proposed method, the response of different laminates subjected to in-plane loading is predicted and compared with experiment results. Predictions are in good agreement with available experimental data. Moreover, the capability of this method for more complicated geometry is shown by predicting matrix crack evolution in a composite plate with open hole under tension.

## 2. Micro model

The micro-scale model characterizes damage in a non-homogenized domain. The domain is discretized using layered SHELL99 elements in ANSYS. The results are stored in a database (DB) of parameters as a function of materials properties ( $E_1$ ,  $E_2$ ,  $G_{12}$ ,  $\nu_{12}$ ) and crack density  $\rho$ . Stress hardening and softening behavior due to matrix cracking is predicted by the micro-model as a function of crack density. The internal parameters, which are calculated a priori by the micro-model are: strain energy release rate  $G_m$ , longitudinal stiffness  $E_{eff}$  and Poisson's ratio  $\nu_{eff}$ . They are stored in the DB in normalized form. The constitutive law for the damaged laminate can be recreated using these previously computed parameters, whenever the macro-model requires it.

To calculate the internal parameters, stress-strain distributions in a properly defined unit-cell or a representative volume element are obtained. The unit-cell is representative of the laminate containing matrix cracking in damaged layers (Fig. 1). FE unit-cell models are

developed to find the stress distribution and internal parameters as a function of crack density. Unit cells are analyzed under in-plane, load control conditions.

The micromechanical unit-cell is a 2D discretized model (Fig. 2). The parameters are obtained from the linear elastic analyses of 2D models with various lengths, where the length  $L$  of the unit cell is related to the crack density  $\rho$  by  $\rho=1/L$ .

Due to symmetry conditions, half of the unit-cell is modeled in the  $x$ - $z$  plane (Fig. 2), using layered SHELL99 elements in ANSYS.

While modeling matrix cracks in a damaged layer ( $\rho_n$ ), other layers are assumed to be undamaged. The external load is applied to un-damaged layers. Damaged layers are free from loading and constraints at the crack faces.

Mesh sensitivity analyses were performed and it showed that using 4 to 6 elements in the thickness direction of each layer leads to acceptable results.

Considering the concept of discrete fracture mechanics <sup>2</sup>, the strain energy release rate can be defined as follows:

$$G_m = \frac{-\Delta U + W_{ext}}{\Delta A} \quad (1)$$

where  $U$  is strain energy of the unit-cell,  $W$  is the external work, and  $A$  is the area of the crack face, which is formed at the specified crack density. To calculate the value of  $G_m$ , a 2D unit-cell subjected to in-plane loading is analyzed using FEA. For this purpose, the following steps are performed.

A unit-cell with the length of  $L$  and crack density of  $1/L$  subjected to tension loading  $\sigma_x$  is considered (Fig. 2.a). The strain energy  $U(L)$  and external work  $W(L)$  are calculated for crack spacing  $L$ . The unit-cell coordinate system is defined in a way that the fibers of the cracked layer are always perpendicular to the  $x$ - $z$  plane. For example, if matrix cracks are investigated in the  $\theta$  lamina of a  $[0_m/\theta_n]_s$  laminate, the unit-cell stacking sequence is  $[(90-\theta)_m/90_n]_s$  in the unit-cell coordinate system.

The same unit-cell but with an internal matrix crack (crack density  $2/L$ , Fig. 2.b) subjected to the same loading is considered to calculate  $U(2L)$  and  $W(2L)$ . Then, the ERR value  $G_m$  is calculated using eq. (1).

This procedure is repeated for various unit-cells with different length (crack density) to calculate the values of  $G_m$  as a function of crack density.

Micrographs of matrix cracks can be seen in Fig. 3.a, for cross-ply laminates. The unit-cell deformation and stress contour are shown in Fig. 3.b, where it is clear that the longitudinal stress is not only a function of  $x$  direction, but, it is also a function of  $z$  direction too.

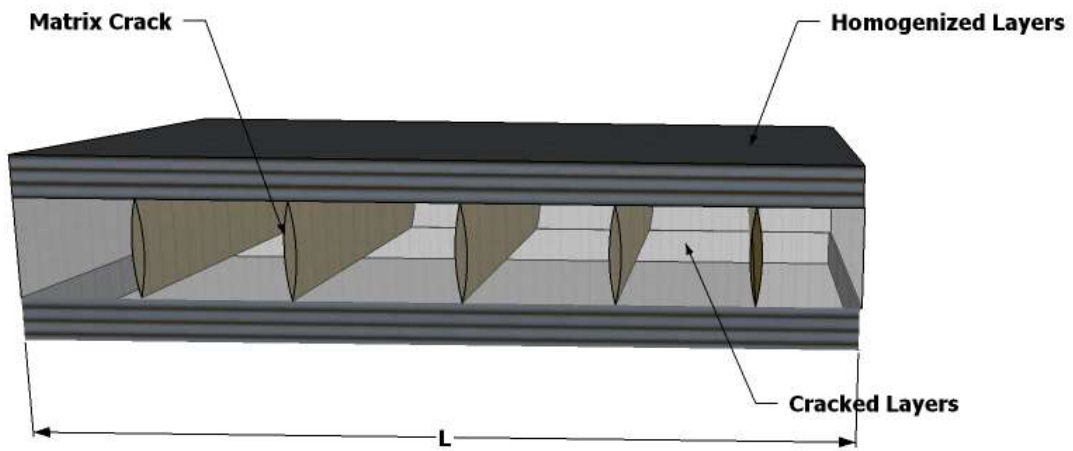


Fig. 1. Micromechanics unit-cell containing matrix cracks.

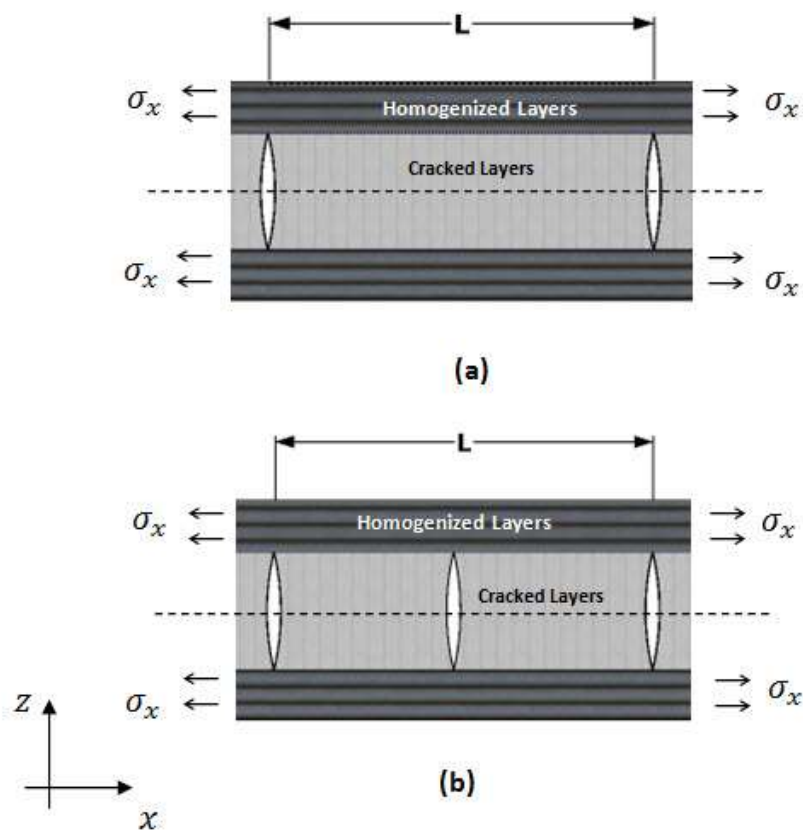
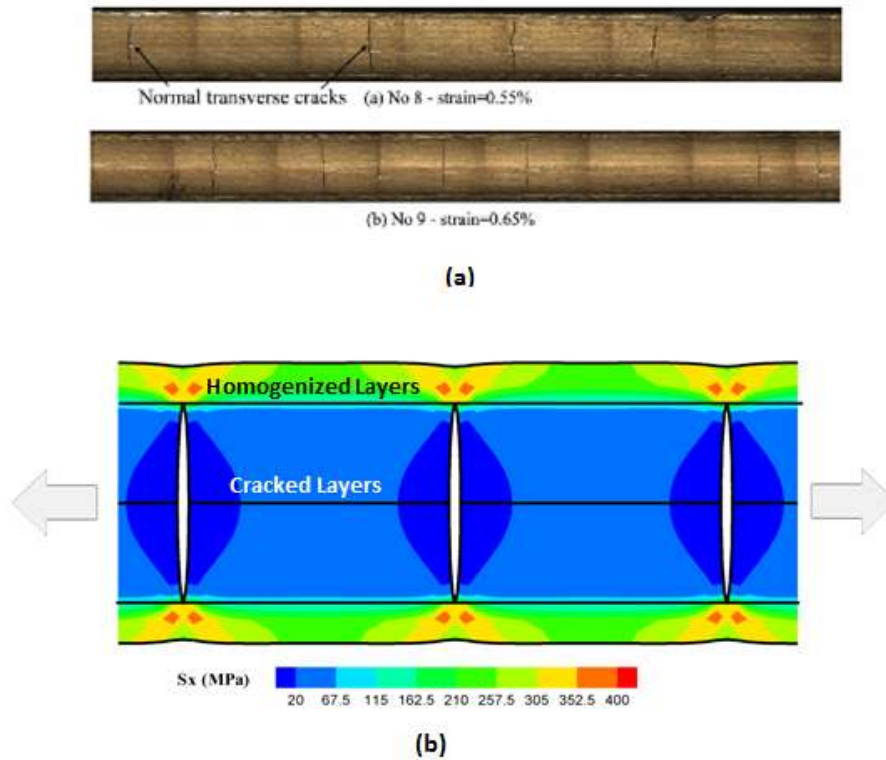


Fig. 2. Geometry and loading of unit-cells, (a) Unit-cell with length of  $L$ , (b) The same unit-cell with a proposed crack in the cracked layer (crack density  $2/L$ ).



**Fig. 3. Matrix cracks in a cross-ply laminate (a) Experimental observation<sup>27</sup> (b) Stress contour in the unit-cell ( $\sigma_x$  (MPa))**

To calculate the stiffness reduction of the laminates due to the matrix cracking, two simple approaches can be used. A one-dimensional stress-strain relation (strain-based)

$$\sigma = E_{eff} \epsilon \quad (2)$$

or a one-dimensional energy balance (energy-based)

$$E_{eff} = \frac{\sigma_x^2}{2U} LBW \quad (3)$$

where,  $L$ ,  $W$  and  $B$ , are the length, width, and thickness of the laminate, respectively. It will be shown in Section 4 that the energy based method results are in better agreement with the experimental results. Therefore, the energy based method is used to calculate the stiffness reduction in the following sections of this paper.

Another effect of matrix cracks on the mechanical properties of laminates is the reduction of Poisson's ratio. Increasing crack density results in decreasing of Poisson's ratio. Several investigations have been performed to study the effects of matrix cracking on reduction of Poisson's ratio<sup>20, 23, 28, 29</sup>. For this purpose, a FE unit-cell is defined to calculate

the reduction of Poisson's ratio as shown in

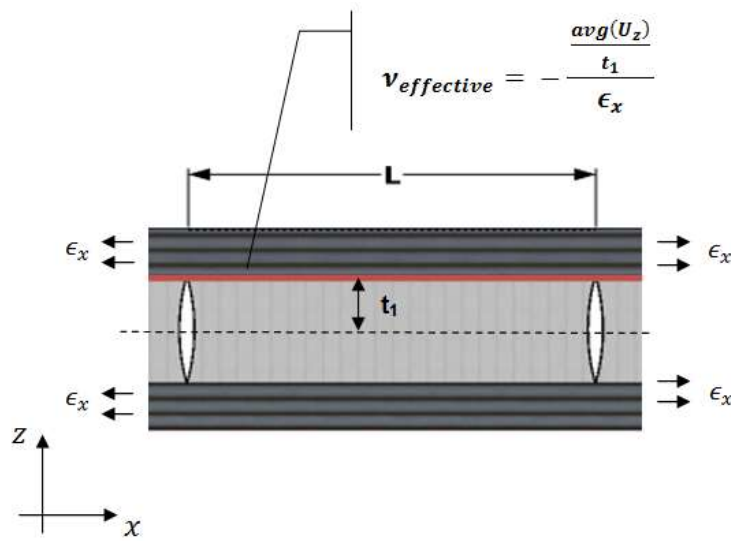


Fig. 4, and the effective Poisson's ratio is calculated as

$$\nu_{eff} = -\frac{avg(u_z)}{\epsilon_x} \quad (4)$$

where  $avg(u_z)$  is the average of displacement in the thickness direction at the interface between un-damaged and damaged layers (red solid line in

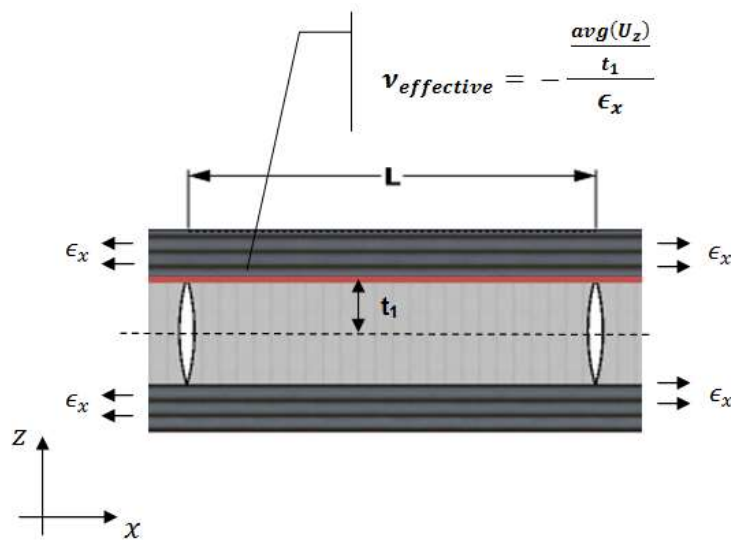
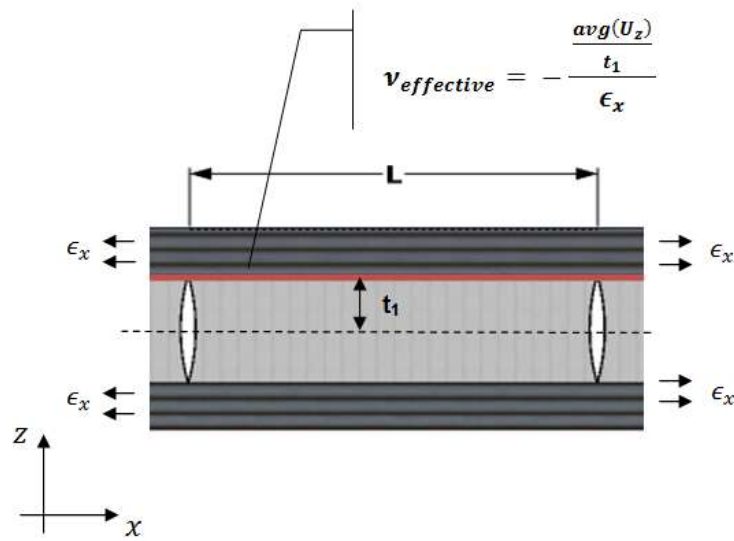


Fig. 4.),  $t_1$  is half of the thickness of damaged layers and  $\epsilon_x$  is the strain applied to the un-



damaged layers (

Fig. 4). Several investigations performed by the authors showed that this definition gives the good results for Poisson's ratio in the cracked Unit-cell. Moreover, this definition is in coincidence with the definition of the Poisson's ratio.

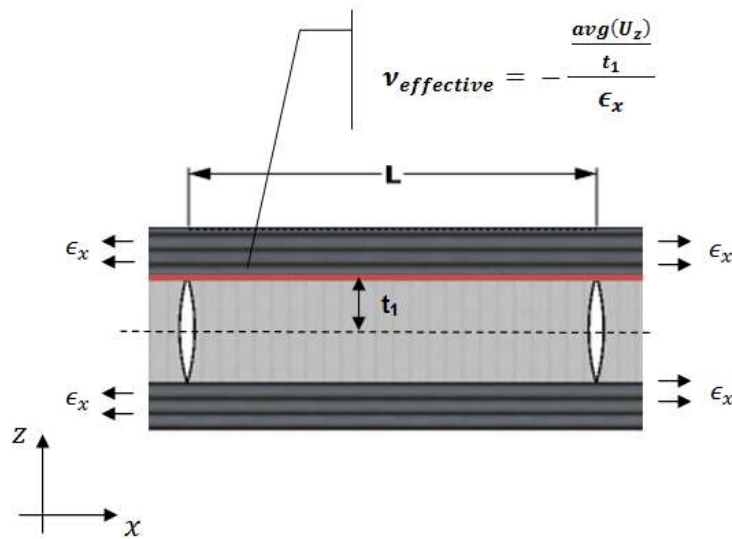


Fig. 4. The unit-cell boundary conditions for prediction of Poisson's ratio.

The normalized strain energy release rate is defined as <sup>6</sup>

$$g_m(\rho) = \frac{G_m(\rho)}{C_3 t_1 \left( \frac{E_2}{E_0} \sigma_{rem} \right)^2} \quad (5)$$

where  $C_3$  is defined as

$$C_3 = \frac{1}{20E_2} + \frac{\lambda}{60E_1} (8\lambda^2 + 20\lambda + 15) \quad (6)$$

$$\lambda = \frac{t_2}{t_1}$$

and  $t_2$  is the thickness of the undamaged layer.

The parameters  $g_m(\rho)$ ,  $E_{\text{eff}}(\rho)/E_0$ ,  $\nu_{\text{eff}}(\rho)/\nu_0$  are stored in the database in normalized form, where  $E_0, \nu_0$  are the longitudinal modulus and major Poisson's ratio of the virgin materials, assumed to have an initial crack density  $\rho = 0.01$  [1/mm], which represents the defects existing in the virgin material. Normalized strain energy release rate, overall stiffness reduction and Poisson's ratio versus crack density are shown in Fig. 5 for several Glass/Epoxy and Carbon/Epoxy cross-ply laminates with material properties given in Table 1. The key important observation for this section is that the parameters are easy to calculate a priori for general laminates as a function of crack density.

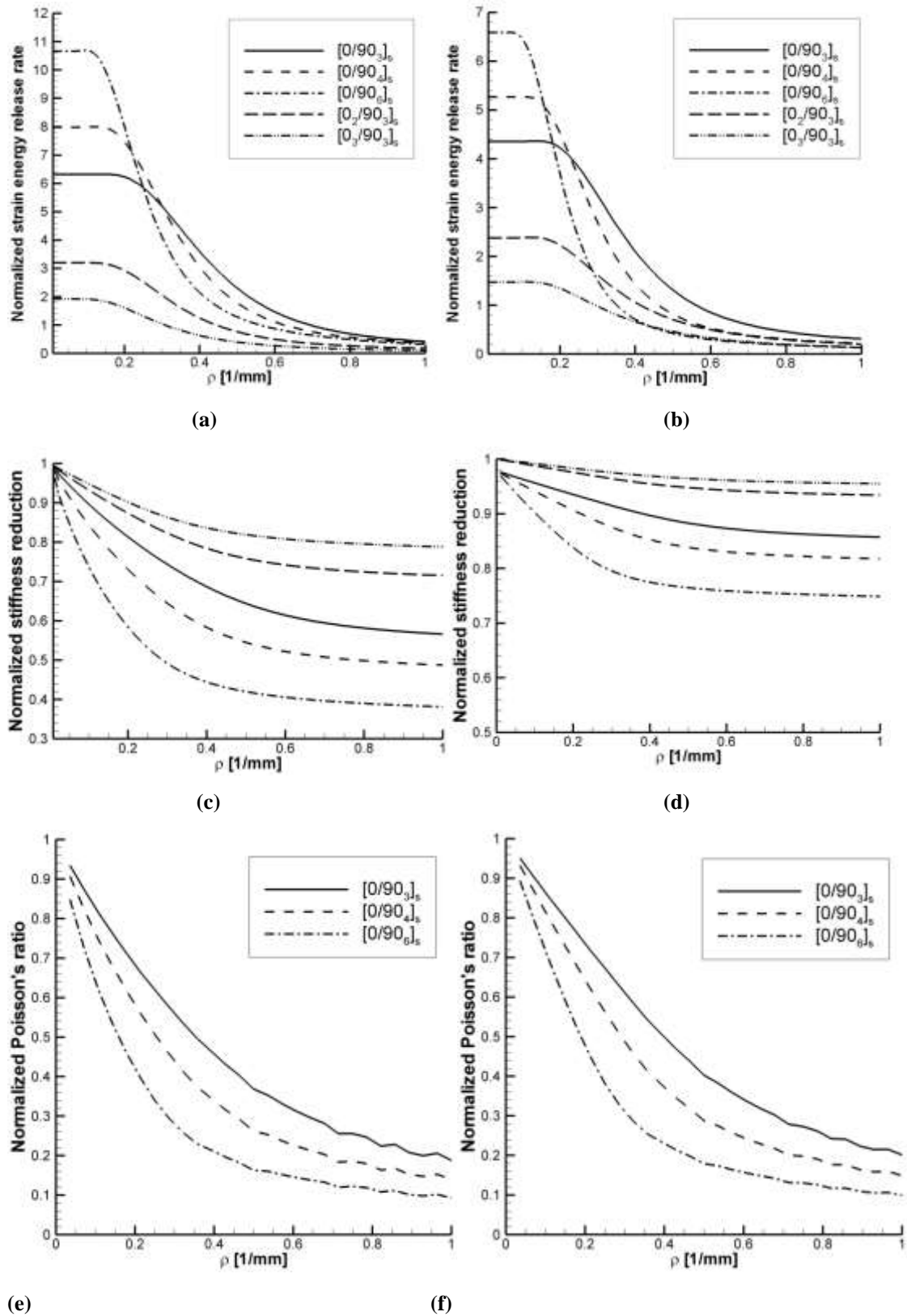


Fig. 5. Graphical view of micro-scale DB, Strain energy release rate versus crack density for (a) Glass/Epoxy, (b) Carbon/Epoxy, and normalized stiffness versus crack density for (c) Glass/Epoxy, and (d) Carbon/Epoxy. (e) Poisson's ratio versus crack density for Glass/Epoxy, and (f) Carbon/Epoxy laminates

**Table 1. Mechanical properties <sup>6</sup>**

Material Properties	Glass/Epoxy	Carbon/Epoxy
<b>E1 (MPa)</b>	41700	128000
<b>E2 (MPa)</b>	13000	7200
<b>G12 (MPa)</b>	3400	4000
<b>G23 (MPa)</b>	4580	2400
<b>v<sub>12</sub></b>	0.3	0.3
<b>v<sub>23</sub></b>	0.42	0.5
<b>Ply thickness (mm)</b>	0.203	0.203
<b>G<sub>c</sub> (J/m<sup>2</sup>)</b>	240	690

### 3. Macro model

#### 3.1. CDM Model

When the strain reaches a critical value (damage onset), matrix cracks initiate in the most vulnerable ply. By increasing the applied load, the crack density increases and causes stiffness reduction in the laminate. Therefore, the macro model is confronted with non-linear constitutive behavior. In the (CDM) approach, the stress-strain relation for such laminate can be presented as

$$[\sigma] = [Q][\epsilon] \quad (7)$$

where

$$Q = [D][T][\bar{Q}] \quad (8)$$

and  $D$  is the damage tensor,  $T$  is the coordinate transformation matrix, and  $\bar{Q}$  is the undamaged stiffness matrix. The damage tensor is defined as

$$[D] = \begin{bmatrix} 1-D_{11} & 1-D_{12} & 0 \\ 1-D_{12} & 1-D_{22} & 0 \\ 0 & 0 & 1-D_{66} \end{bmatrix} \quad (9)$$

For undamaged in plane stress condition, the  $\bar{Q}$  matrix can be calculated from

$$[\bar{Q}] = \begin{bmatrix} \frac{E_1}{(1-\nu_{12}\nu_{21})} & \frac{E_2\nu_{12}}{(1-\nu_{12}\nu_{21})} & 0 \\ \frac{E_2\nu_{12}}{(1-\nu_{12}\nu_{21})} & \frac{E_2}{(1-\nu_{12}\nu_{21})} & 0 \\ 0 & 0 & G_{12} \end{bmatrix} \quad (10)$$

For example, the stress-strain relation eq. (7) of 90° layers is calculated according to

$$\begin{Bmatrix} \sigma_x \\ \sigma_z \\ \tau_{xz} \end{Bmatrix} = \begin{bmatrix} \frac{(1-d_E)E_2}{(1-\nu'_{12}\nu'_{21})} & \frac{(1-d_E)\nu'_{12}E_2}{(1-\nu_{12}\nu_{21})} & 0 \\ \frac{(1-d_E)\nu'_{12}E_2}{(1-\nu'_{12}\nu'_{21})} & \frac{(1-d_E)E_2}{(1-\nu'_{12}\nu'_{21})} & 0 \\ 0 & 0 & (1-d_E)G_{12} \end{bmatrix} \begin{Bmatrix} \epsilon_x \\ \epsilon_z \\ \gamma_{xz} \end{Bmatrix} \quad (11)$$

Therefore, the degraded Poisson's ratios are calculated as follows:

$$\begin{aligned} \nu'_{23} &= (1-d_\nu)\nu_{23} \\ \nu'_{32} &= \frac{E_3}{(1-d_E)E_2}\nu'_{23} \\ \nu'_{12} &= \frac{E_1}{(1-d_E)E_2}\nu_{12} \\ \nu'_{21} &= \frac{(1-d_E)E_2}{E_1}\nu_{12} \end{aligned} \quad (12)$$

where,  $d_E$ ,  $d_\nu$ , are the damage parameters representing stiffness and Poisson's ratio reduction, respectively. They are formally defined as,

$$d_E = \frac{E_{2eff}}{E_2} \quad (13)$$

$$(d_\nu)_{ij} = \frac{\nu_{ijeff}}{\nu_{ij}} \quad (14)$$

It should be noted that, in this approach damage parameters are directly applied to the material properties. Thus damage tensor is not defined independently and it is merged into

the stiffness matrix. Moreover, damage parameter in lamina embedded in a laminates never reaches 1. Because even very densely cracked layers still contribute in load carrying and their effective stiffness cannot be completely ignored. In other word, the assumption  $d < 1$  is only upper limit and does not necessarily means that  $d$  becomes eventually 1. Having the damage parameters the stress components are calculated in the macro modeling. For this purpose, a damage surface is required to find an equilibrium condition for the structure under loading.

### 3.2. Damage surface

At this point, an evolution law to describe the evolution of damage is necessary. As explained in the previous sections, micromechanics approaches have the capability to obtain the strain energy release rate and reduced stiffness as a function of crack density<sup>2</sup>. In the present study, the evolution of the damage state is predicted by comparing the obtained strain energy release rate with the fracture toughness. Therefore, a damage surface is defined such that initiation damage does not occur as long as

$$f_m = G_m - G_{Ic} < 0 \quad (15)$$

where  $G_{Ic}$  is critical strain energy release rate in mode-I fracture and  $f_m$  is the damage surface.

Crack density  $\rho$  is the only parameter that is transferred from the macro-model to the micro-model. Then, the stiffness and Poisson's ratio reduction ( $d_E$  and  $d_v$ ) are returned from the micro- to the macro-model. At each crack density, the values of  $d_E$  and  $d_v$  are calculated using (13) and (14) from the results of the micro-model. A procedure to find the crack density at each loading step is needed. The value of  $G_m$  for each crack density is a function of unit-cell remote stress  $\sigma_{rem}$ , which is a function of the damage value. Therefore, the damage surface behaves nonlinearly and a return mapping algorithm (RMA) is required.

At each loading step, the crack density  $\rho_c$  is obtained such that  $G = G_c$  with updated values of  $d_E$ ,  $d_v$ , and stress field. Having  $\rho_c$ , the updated damage parameters ( $d_E$  and  $d_v$ ) can be obtained from the micro-data database.

For this purpose, an ANSYS *usermaterial* routine has been developed to calculate the value of crack density and damage at each gauss point of damaged layers and at each loading step. A flow chart is shown in Fig. 6.

The structural analysis program (ANSYS) interacts with the *usermaterial* as follows. The main input to the *usermaterial* is the strain  $\epsilon$ . The output is the tangent stiffness of the material  $dC/dE$  and the stress  $\sigma(\epsilon)$ . The crack density  $\rho$  is stored as a stable variable for each Gauss Point to remember the state of damage at the point. Therefore, the *usermaterial* is a numerical constitutive model for  $\sigma(\epsilon)$ , and  $dC/dE$ .

The objective of the damage evolution algorithm is to find the value of  $\rho$  that results in a value of degraded stiffness tensor  $C(\rho)$  such that  $\sigma$  is in equilibrium at the Gauss point. Since  $f(\rho)$  in (15) must be semi-definite negative (cannot be  $f > 0$  under no circumstance), a RMA is used to find  $\Delta\rho$  iteratively until  $f \leq 0$ <sup>2</sup>.

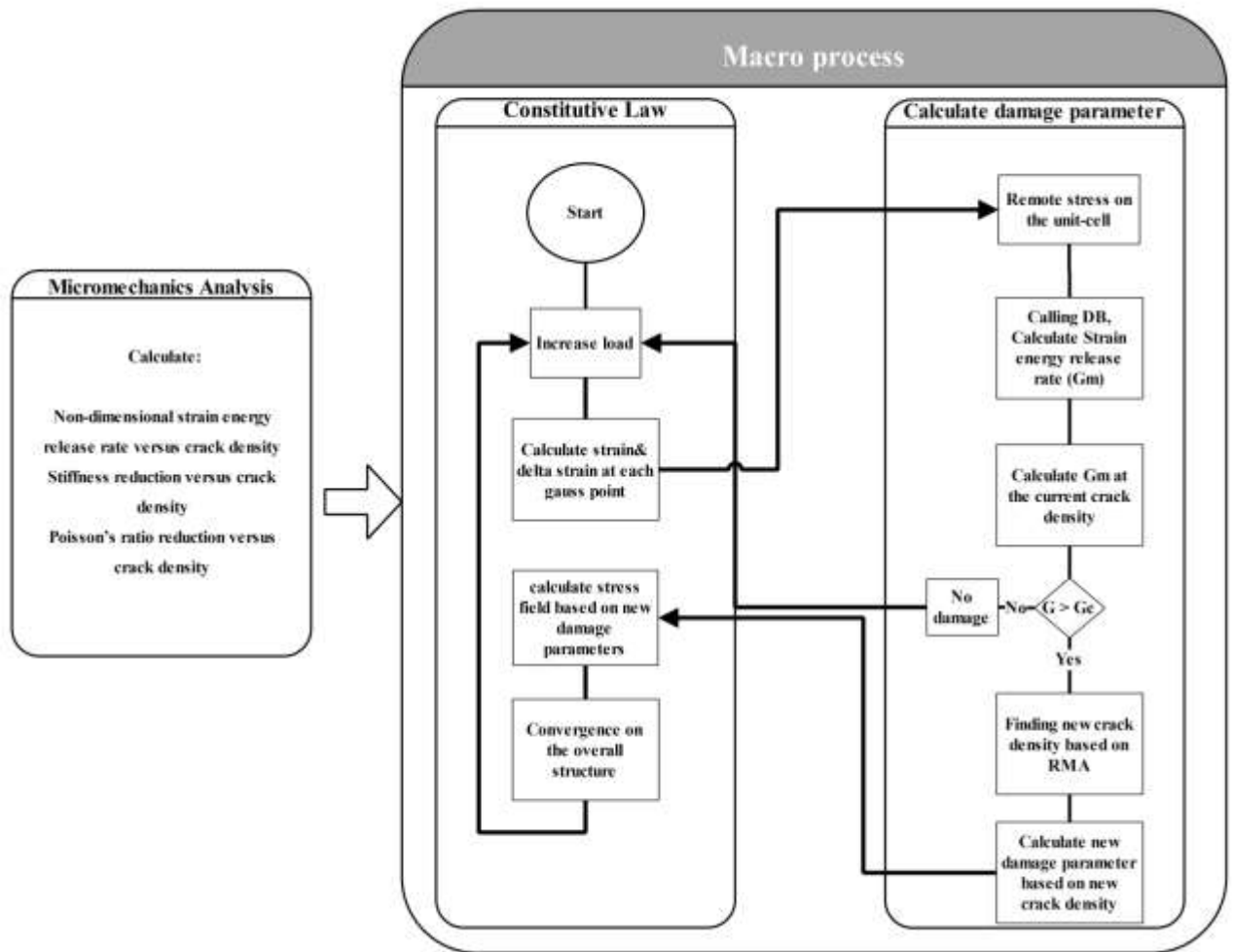


Fig. 6. Flowchart of the FE-based micro/macro scale method

About 100 elastic analyses on a cracked unit-cell were performed for various unit-cell lengths (crack densities). The results of these micromechanics analyses (normalized strain energy release rate, normalized stiffness reduction, and normalized Poisson's ratio versus crack density) are stored as a database curves. This means that the micromechanics model is reduced to an interpolation procedure between the micromechanics data. The number of available data points in the micromechanics database may affect the convergence of the macro results. Stress versus strain are shown in Fig. 7 for two micromechanics databases containing 50 and 100 points for  $0 < \rho < 1.0$ . No oscillations were observed when using 100 data points, but oscillations were observed using 50 data points as shown.

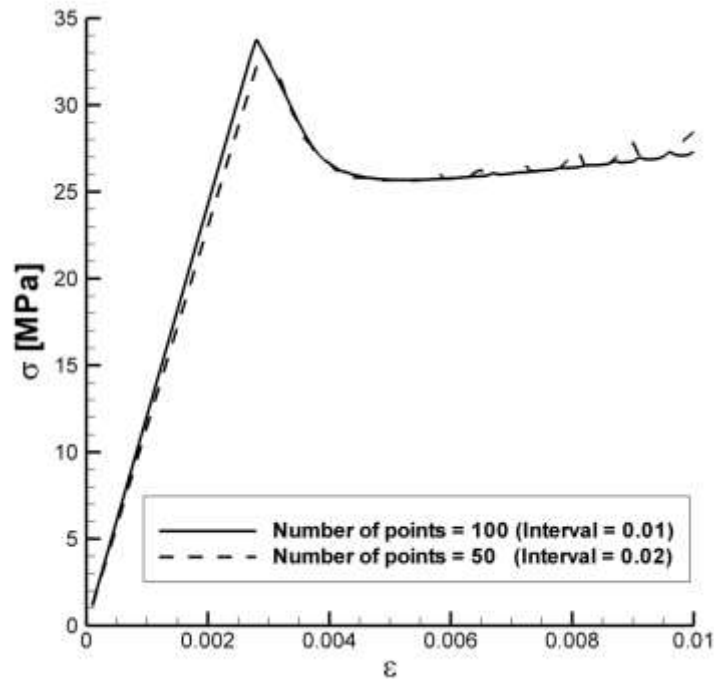


Fig. 7. Effect of number of micromechanics data points on stress-strain prediction.

#### 4. Results and Discussion

To verify the proposed model, predicted stiffness and matrix crack evolution are compared with several available experimental data and numerical results. Material properties are shown in Table 2. An initial crack density  $\rho = 0.01$  was used for all models.

Comparison of the predicted stiffness versus crack density is shown in Fig. 8 using both strain based (eq. 2) and energy based (eq. 3) definitions, with experimental results for a  $[0/90_3]_s$  Glass/Epoxy laminate with material properties given in Table 2<sup>30</sup>. It can be seen that the energy based method is more accurate. Therefore, the energy based method is used for predicting the stiffness in this study.

Table 2. Mechanical properties.

Material Properties	Lim & Hong <sup>30</sup>	Varna et al. <sup>31</sup>	High Smith <sup>29</sup>	O. Higgins et al. <sup>33</sup>
E1 (MPa)	144780	44700	41700	138000
E2 (MPa)	9580	12700	13000	10000
G12 (MPa)	4790	5800	3400	5200
G23 (MPa)	9580	4500	4580	3690*
$\nu_{12}$	0.31	0.297	0.3	0.3
$\nu_{23}$	0.5	0.41	0.42	0.5*
Ply thickness (mm)	0.13	0.144	0.203	0.203*
$G_c$ (J/m <sup>2</sup> )	130	175	240	150*

\* Estimated parameters

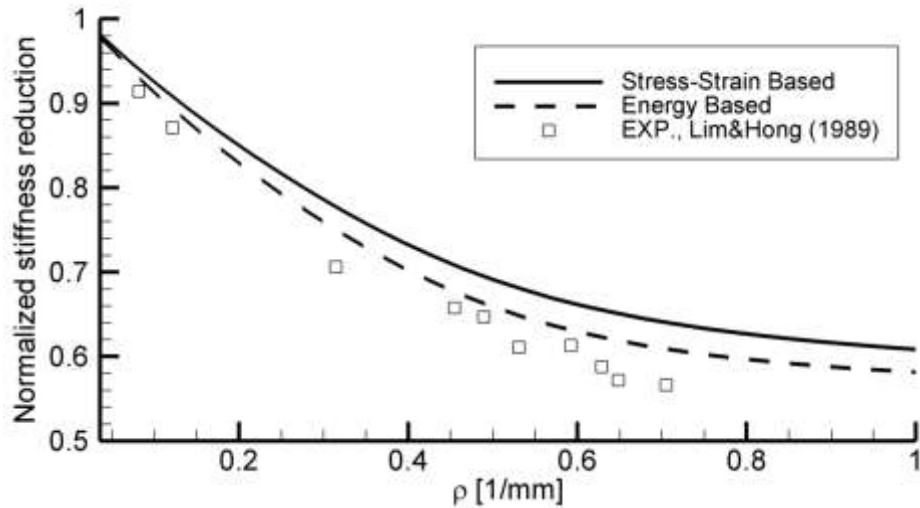


Fig. 8. Stiffness versus crack density for  $[0/90_3]_s$  Glass/Epoxy laminate <sup>31</sup>.

Predicted normalized Poisson’s ratio versus crack density is compared in Fig. 9 with the available experimental <sup>23</sup> and numerical results <sup>20</sup>, with material properties given in Table 2<sup>32</sup>. It is observed that the predicted Poisson’s ratio reductions in this study are in good agreement with the experimental results and they are more conservative than those predicted by the method presented in <sup>20</sup>. In other word, the proposed model for prediction of Poisson’s ratio gives the lower bound of the results.

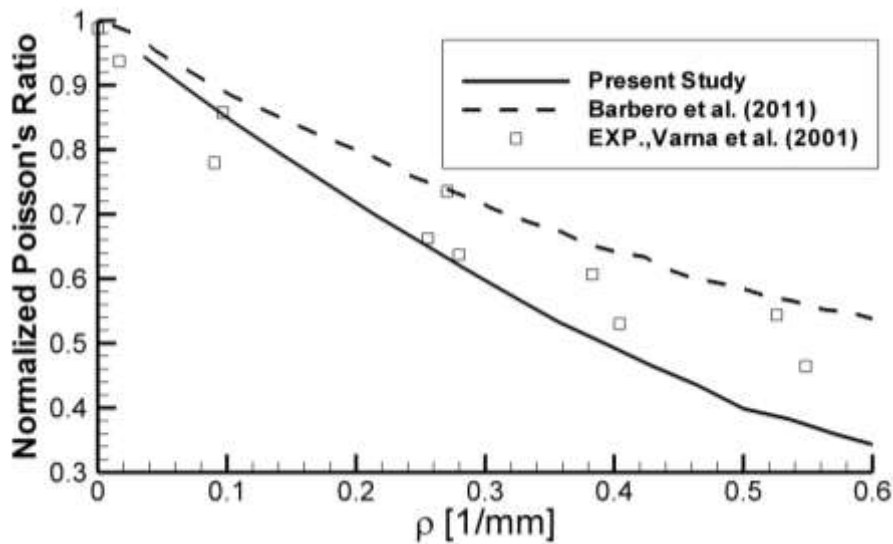


Fig. 9. Poisson’s ratio versus crack density for  $[0_2/90_4]_s$  Glass/Epoxy <sup>20, 23</sup>.

Predicted stiffness reduction and crack density versus remote stress are compared with the available experimental results in Fig. 10for  $[0/90_3]_s$  Glass/epoxy laminate for material properties given in Table 2 <sup>30</sup>. The predicted elastic moduli are in acceptable agreement with

the experimental data. It should be noted that, considering initial crack density, the normalized stiffness reduction would not initiate from 1.0. In other word, it is assumed that the laminate has an initial damage in accordance with the initial crack density. Thus, at the first load step, damage does not growth till the strain energy release rate reaches the critical strain energy release rate ( $G_{Ic}$ ).

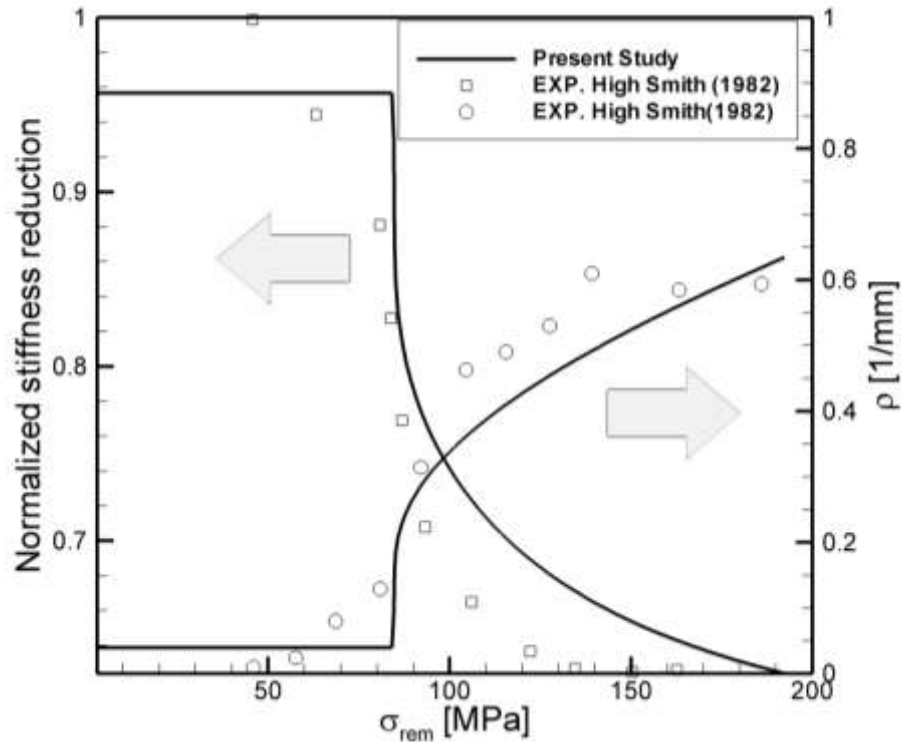


Fig. 10. Stiffness and crack density versus remote stress for  $[0/90_3]_s$  Glass/Epoxy<sup>30</sup>.

The capability of this method for matrix cracking of Carbon/Epoxy laminates is also examined. Predicted normalized stiffness versus crack density is compared with available experimental data for several AS4-3502 Carbon/Epoxy cross-ply laminates (with material properties given in Table 2) in Fig. 11. The obtained good agreements between predicted and experimental data are shown. Comparison of the results in **Error! Reference source not found.** Fig. 10 and Fig. 11, it is indicated that the matrix crack saturation will occur at larger crack density in Carbon/epoxy laminates rather than Glass/Epoxy. In contrast, Carbon/Epoxy laminates experiences lower stiffness reduction. Because the ratio of  $E_2/E_1$  is relatively very small.

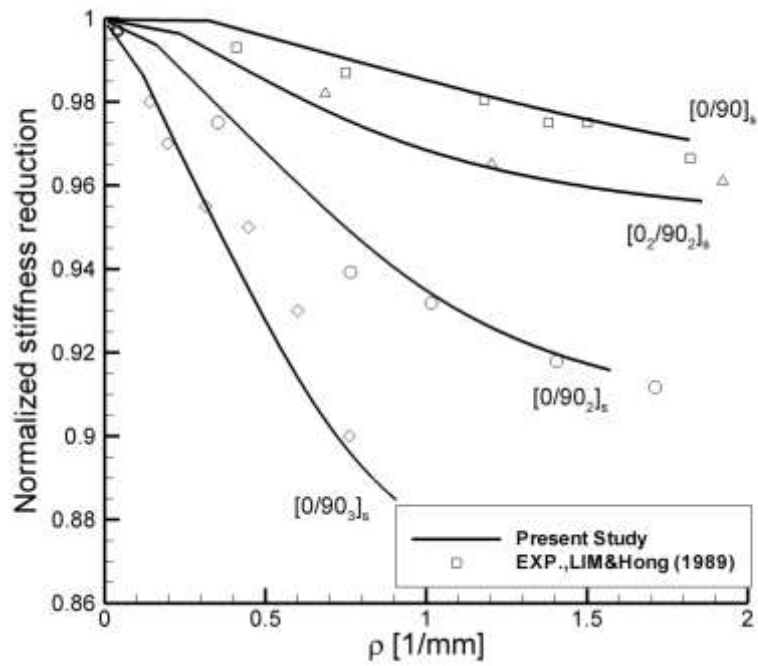


Fig. 11. Stiffness versus crack density for AS4-3502 Carbon/Epoxy <sup>31</sup>.

Normalized stiffness versus applied strain for a  $[0_2/90_4]_s$  Glass/Epoxy laminate with material properties given in Table 2 <sup>32</sup> are compared with experimental data and reference <sup>20</sup> in Fig. 12. It is observed that the developed model predicts more stiffness reduction at the beginning of the damage development in comparison with the experimental results. It means that the model predicts more conservative stiffness reduction.

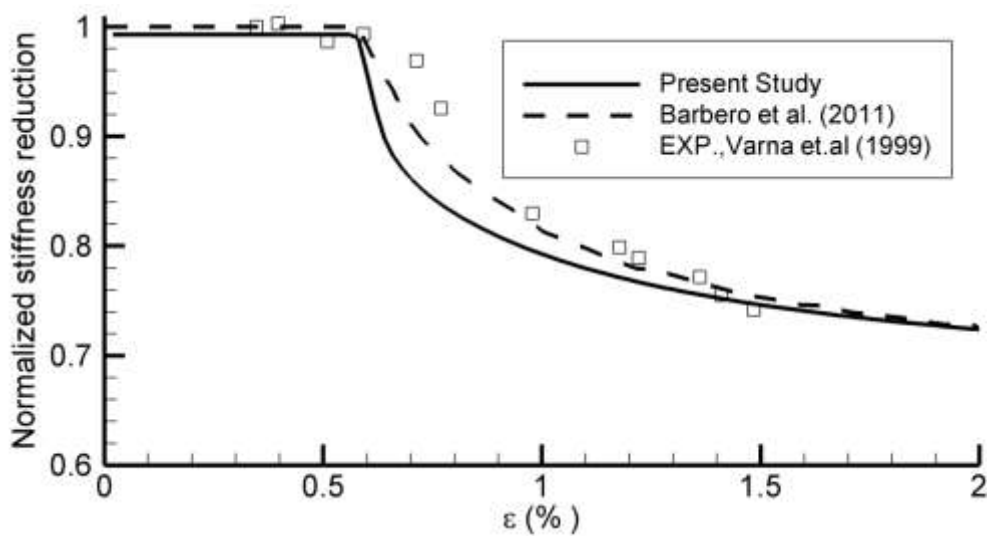


Fig. 12. Stiffness versus applied strain (%) for  $[0_2/90_4]_s$  Glass/Epoxy <sup>20, 32</sup>

Crack density growth in  $[0/+θ/-θ/0_{1/2}]_s$  laminates is also predicted for Glass/Epoxy laminates Fig. 13 to Fig. 15 show the crack density versus applied strain for  $[0/90_8/0_{1/2}]_s$ ,  $[0/+70_4/-70_4/0_{1/2}]_s$  and  $[0/55_4/-55_4/0_{1/2}]_s$  laminates respectively. For the same material, the predicted results are in good agreement with the numerical<sup>21</sup> and experimental results. It is evident that crack density is initiated at higher applied strain for  $[0/55_4/-55_4/0_{1/2}]_s$  laminate. Similarly, saturation has occurred at higher applied strains for this laminate.

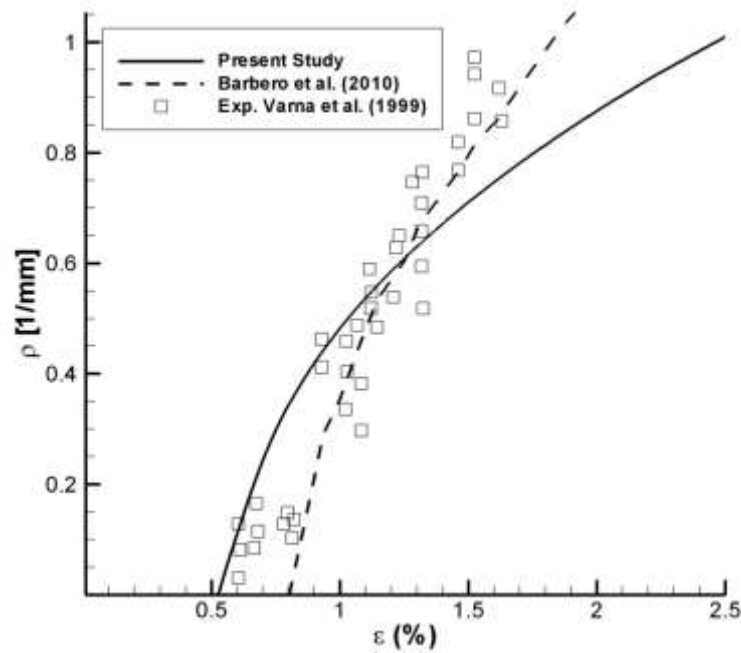


Fig. 13. Crack density versus applied strain for  $[0/90_8/0_{1/2}]_s$  Glass/Epoxy<sup>21, 32</sup>.

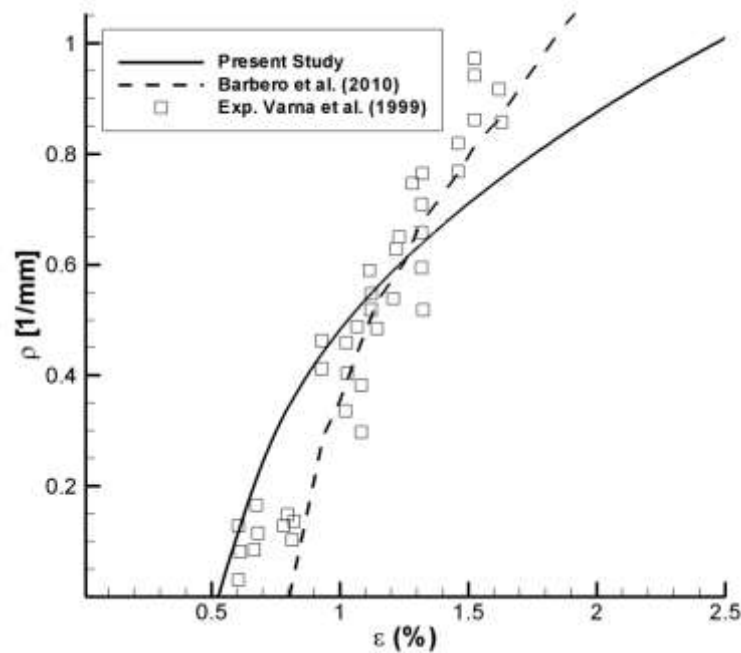


Fig. 14. Crack density versus applied strain for  $[0/+70_4/-70_4/0_{1/2}]_s$  Glass/Epoxy<sup>2, 32</sup>.

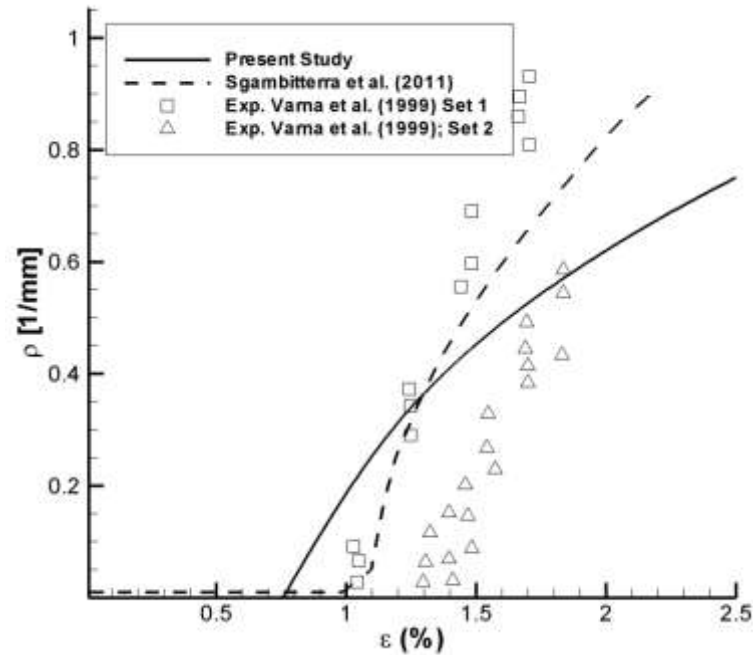


Fig. 15. Crack density versus applied strain for  $[0/+55_4/-55_4/0_{1/2}]_s$  Glass/Epoxy<sup>21, 32</sup>.

Predicted stiffness, Poisson's ratio, and matrix crack evolution using the presented approach are in good agreement with available experimental data for various cross-ply laminates in Fig. 8 to 15.

Next, the capability of the proposed model for progressive damage analyses of complex geometries is evaluated by predicting the matrix crack evolution for  $[90_2/0_2]_s$  CFRP laminate with open hole under tension (OHT) and comparing the results with the experimental observations. Fig. 16 shows the specimen geometry of CFRP OHT with material properties given in Table 2<sup>33</sup>. The specimen is 300 mm long, 36 mm wide and the diameter of the hole is 6 mm.

For this purpose, ANSYS SHELL181 element and the developed usermaterial routine were used. Matrix crack evolution at each integration point of the laminate was calculated and the corresponding crack density was extracted.

Fig. 17.a shows the experimental observation of the damage evolution around the hole. The split crack initiating from the edge of the hole at  $0^\circ$  plies is the first damage<sup>33</sup>. As the load increases, matrix cracks evolve in the  $90^\circ$  plies around the hole towards the outside of the plate. The proposed multi-scale approach has been used to predict matrix cracking in the  $90^\circ$  and the split in the  $0^\circ$  layers. Because of the symmetric conditions, only a quarter of the OHT is modeled. Fig. 17.b. shows the predicted matrix crack density in  $90^\circ$  plies at the load 560 MPa where the matrix cracking has been saturated. As can be seen, the pattern of the matrix crack growth in the developed model is in good agreement with the experimental results. Moreover, the obtained damage corresponding to the split in  $0^\circ$  plies is shown in Fig. 17.c. It should be noted that, the proposed multi-scale damage model is a continuum damage model to predict the average stiffness reduction due to multiple cracks in composite laminates and it

is not theoretically designed for predicting the split. Thus, an intensely damaged area rather than a single discontinuous crack has been predicted by the model. The simulated damage pattern in both  $90^\circ$  and  $0^\circ$  layers are similar to the X-ray experimental results and it is evident that, this model is able to predict the split cracks growth in  $0^\circ$  plies and matrix cracks in  $90^\circ$  plies in more complex structures.

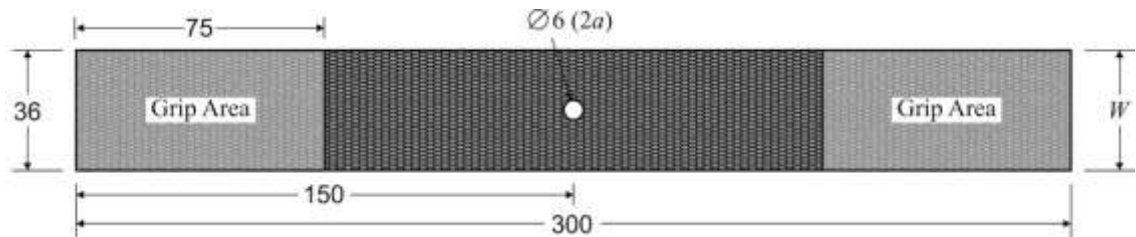
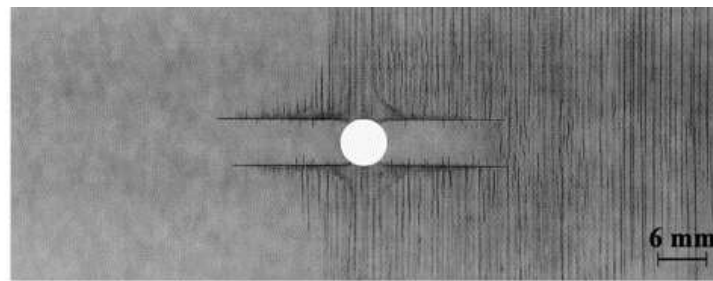
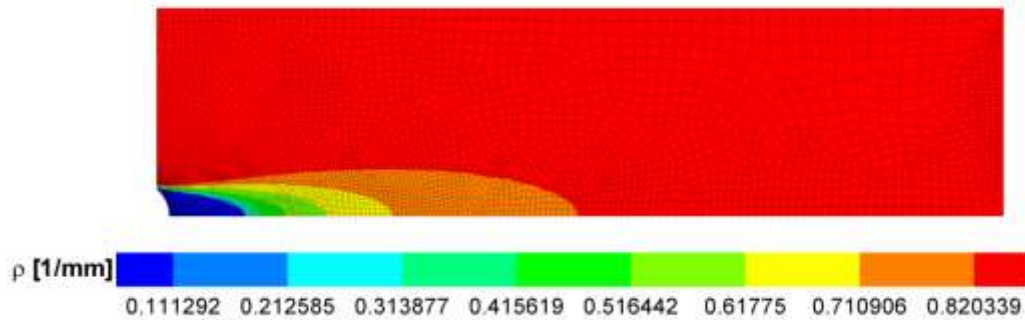


Fig. 16. Open hole tension specimen geometry <sup>33</sup>



(a)



(b)



(c)

Fig. 17 (a). Split & Matrix crack at  $[90_2/0_2]_s$  CFRP laminate at 65%  $S_{OHT}$  ( $S_{OHT} = 860$  MPa) <sup>33</sup>, (b) crack density at  $90^\circ$  plies (c) Split crack evolution in  $0^\circ$  plies

## 5. Conclusions

A simple micro-macro FE based procedure was developed for progressive matrix crack analyses of laminates. Using this method, it is not necessary to execute a complex micromechanics model coupled with the macro-model. The macro-model obtains the constitutive response from the micro-model using a simple interpolation of the micro-data obtained earlier from a parametric FEA of a unit cell, with crack density as the only parameter. The procedure was integrated within ANSYS software.

Predicted stiffness and Poisson's ratio of the damaged laminates are in good agreement with available experimental data for several laminates, indicating that the proposed method is effective and reliable for progressive damage analyses of such laminates. Furthermore, the capability of the model for complex stress state is examined with the damage growth analysis of OHT and comparing the result with the experimental observations.

Future work entails developing unit cells for cracks in angle-ply and other configurations, to use the micro-model to store the associated parameter DB, and to use the DB to exercise the macro-model with complex laminates and loading conditions. Furthermore, exercise those unit cells with  $\sigma = 0$ ,  $\Delta T = 1$  in order to use the macro-model to calculate CTE.

A drawback of the proposed method is that the DB must be populated for every material system and LSS anticipated to be used in practice. This problem is not as severe as it seems, because at least in the Aircraft industry, the number of certified material systems are limited to a few. Also, ply thicknesses are quite consistent in the industry and LSS choices are limited by availability of "building block" experimental data. Furthermore, populating the DB can be automated, and it is done a priori, once and for all.

## References

1. Liu PF and Zheng JY. Recent developments on damage modeling and finite element analysis for composite laminates: A review. *Materials & Design*. 2010; 31: 3825-34.
2. Barbero EJ and Cortes DH. A mechanistic model for transverse damage initiation, evolution, and stiffness reduction in laminated composites. *Composites Part B: Engineering*. 2010; 41: 124-32.
3. Hashin Z. Finite thermoelastic fracture criterion with application to laminate cracking analysis. *Journal of the Mechanics and Physics of Solids*. 1996; 44: 1129-45.
4. Barbero EJ and Makkapati S. Robust design optimization of composite structures. *45th International SAMPE Symposium and Exhibition*. Long Beach, CA, USA, 2000, p. 1341-52.
5. Hashin Z. Analysis of cracked laminates: a variational approach. *Mechanics of Materials*. 1985; 4: 121-36.
6. Nairn JA. The Strain Energy Release Rate of Composite Microcracking: A Variational Approach. *Journal of Composite Materials*. 1989; 23: 1106-29.
7. Vinogradov V and Hashin Z. Variational analysis of cracked angle-ply laminates. *Composites Science and Technology*. 2010; 70: 638-46.
8. Nairn JA and Hu S. The initiation and growth of delaminations induced by matrix microcracks in laminated composites. *International Journal of Fracture*. 1992; 57: 1-24.
9. Nairn JA and Hu S. The formation and effect of outer-ply microcracks in cross-ply laminates: A variational approach. *Engineering Fracture Mechanics*. 1992; 41: 203-21.
10. Okabe T, Sekine H, Noda J, Nishikawa M and Takeda N. Characterization of tensile damage and strength in GFRP cross-ply laminates. *Materials Science and Engineering: A*. 2004; 383: 381-9.
11. Jalalvand M, Hosseini-Toudeshky H and Mohammadi B. Numerical modeling of diffuse transverse cracks and induced delamination using cohesive elements. *Proceedings of the Institution of Mechanical Engineers, Part C: Journal of Mechanical Engineering Science*. 2012.
12. Jalalvand M, Hosseini-Toudeshky H and Mohammadi B. Homogenization of diffuse delamination in composite laminates. *Composite Structures*. 2013; 100: 113-20.
13. Yokozeki T, Aoki T and Ishikawa T. Transverse Crack Propagation in the Specimen Width Direction of CFRP Laminates under Static Tensile Loadings. *Journal of Composite Materials*. 2002; 36: 2085-99.
14. Ladevèze P. A damage computational method for composite structures. *Computers & Structures*. 1992; 44: 79-87.
15. Ladevèze P and Lubineau G. On a damage mesomodel for laminates: micro-meso relationships, possibilities and limits. *Composites Science and Technology*. 2001; 61: 2149-58.
16. Farrokhhabadi A, Hosseini-Toudeshky H and Mohammadi B. Damage analysis of laminated composites using a new coupled micro-meso approach. *Fatigue & Fracture of Engineering Materials & Structures*. 2010; 33: 420-35.
17. Farrokhhabadi A, Hosseini-Toudeshky H and Mohammadi B. A generalized micromechanical approach for the analysis of transverse crack and induced delamination in composite laminates. *Composite Structures*. 2011; 93: 443-55.
18. Hosseini-Toudeshky H, Farrokhhabadi A and Mohammadi B. Consideration of concurrent transverse cracking and induced delamination propagation using a generalized micro-meso approach and experimental validation. *Fatigue & Fracture of Engineering Materials & Structures*. 2012; 35: 885-901.
19. Mohammadi B, Hosseini-Toudeshky H and Sadr-Lahidjani MH. Progressive damage analyses of angle-ply laminates exhibiting free edge effects using continuum damage mechanics with layer-wise finite element method. *Fatigue & Fracture of Engineering Materials & Structures*. 2008; 31: 549-68.
20. Barbero EJ, Sgambitterra G, Adumitroaie A and Martinez X. A discrete constitutive model for transverse and shear damage of symmetric laminates with arbitrary stacking sequence. *Composite Structures*. 2011; 93: 1021-30.
21. Sgambitterra G, Adumitroaie A, Barbero EJ and Tessler A. A robust three-node shell element for laminated composites with matrix damage. *Composites Part B: Engineering*. 2011; 42: 41-50.

22. Moure MM, Sanchez-Saez S, Barbero E and Barbero EJ. Analysis of damage localization in composite laminates using a discrete damage model. *Composites Part B: Engineering*. 2014; 66: 224-32.
23. Varna J, Joffe R and Talreja R. A synergistic damage-mechanics analysis of transverse cracking in  $[\pm 0/90]_s$  laminates. *Composites Science and Technology*. 2001; 61: 657-65.
24. Singh CV and Talreja R. A synergistic damage mechanics approach for composite laminates with matrix cracks in multiple orientations. *Mechanics of Materials*. 2009; 41: 954-68.
25. Sadeghi G, Hosseini-Toudeshky H and Mohammadi B. In-plane progressive matrix cracking analysis of symmetric cross-ply laminates with holes. *Fatigue & Fracture of Engineering Materials & Structures*. 2014; 37: 290-305.
26. Sadeghi G, Hosseini-Toudeshky H and Mohammadi B. An investigation of matrix cracking damage evolution in composite laminates – Development of an advanced numerical tool. *Composite Structures*. 2014; 108: 937-50.
27. Jalalvand M, Wisnom MR, Hosseini-Toudeshky H and Mohammadi B. Experimental and numerical study of oblique transverse cracking in cross-ply laminates under tension. *Composites Part A: Applied Science and Manufacturing*. 2014; 67: 140-8.
28. Hashin Z. Analysis of Orthogonally Cracked Laminates Under Tension. *Journal of Applied Mechanics*. 1987; 54: 872-9.
29. Kashtalyan M and Soutis C. Analysis of local delaminations in composite laminates with angle-ply matrix cracks. *International Journal of Solids and Structures*. 2002; 39: 1515-37.
30. High Smith A. Stiffness Reduction Mechanisms in Composite Laminates. *Damage in Composite Materials*. 1982; ASTM STP 775: 15.
31. Lim SG and Hong CS. Effect of transverse cracks on the thermomechanical properties of cross-ply laminated composites. *Composites Science and Technology*. 1989; 34: 145-62.
32. Varna J, Joffe R, Akshantala NV and Talreja R. Damage in composite laminates with off-axis plies. *Composites Science and Technology*. 1999; 59: 2139-47.
33. O'Higgins RM, McCarthy MA and McCarthy CT. Comparison of open hole tension characteristics of high strength glass and carbon fibre-reinforced composite materials. *Composites Science and Technology*. 2008; 68: 2770-8.